

Kinematics of geodesic flows in stringy black hole backgrounds

Anirvan Dasgupta*

Department of Mechanical Engineering and Centre for Theoretical Studies, Indian Institute of Technology, Kharagpur 721 302, India

Hemwati Nandan†

Centre for Theoretical Studies, Indian Institute of Technology, Kharagpur 721 302, India

Sayan Kar‡

Department of Physics and Centre for Theoretical Studies, Indian Institute of Technology, Kharagpur 721 302, India

(Received 13 December 2008; published 5 June 2009)

We study the kinematics of timelike geodesic congruences in two and four dimensions in spacetime geometries representing stringy black holes. The Raychaudhuri equations for the kinematical quantities (namely, expansion, shear, and rotation) characterizing such geodesic flows are written down and subsequently solved analytically (in two dimensions) and numerically (in four dimensions) for specific geodesic flows. We compare between geodesic flows in dual (electric and magnetic) stringy black hole backgrounds in four dimensions, by showing the differences that arise in the corresponding evolutions of the kinematic variables. The crucial role of initial conditions and the spacetime curvature on the evolution of the kinematical variables is illustrated. Some novel general conclusions on caustic formation and geodesic focusing are obtained from the analytical and numerical findings. We also propose a new quantifier in terms of the time (affine parameter) of approach to a singularity, which may be used to distinguish between flows in different geometries. In summary, our quantitative findings bring out hitherto unknown features of the kinematics of geodesic flows, which, otherwise, would have remained overlooked, if we confined ourselves to only a qualitative analysis.

DOI: [10.1103/PhysRevD.79.124004](https://doi.org/10.1103/PhysRevD.79.124004)

PACS numbers: 04.20.Cv, 04.40.-b, 83.10.Bb, 97.60.Lf

I. INTRODUCTION

The kinematics of geodesic congruences is characterized by three kinematical quantities: isotropic expansion, shear, and rotation (henceforth referred as ESR) [1–6]. The evolution of these quantities along the geodesic flow, are obtained from the Raychaudhuri equations [1–6]. These equations are derived by relating the evolution of the deformation (or deviation) vector between two neighboring geodesics (expressed in terms of the ESR variables) to the curvature of the space/spacetime. This is already a well-studied subject (see [6] and the references therein).

In its original incarnation, the Raychaudhuri equation provided the basis for the description and analysis of spacetime singularities in gravitation and cosmology [7]. For example, the equation for the expansion and the resulting theorem on geodesic focusing is a crucial ingredient in the proofs of Penrose-Hawking singularity theorems [8,9]. However, these equations have a much wider scope in studying geodesic as well as nongeodesic flows in nature which may possibly arise in diverse contexts (see [6] for some open issues). We have recently used these equations to investigate the kinematics of flows on flat and curved deformable media (including elastic and viscoelastic media) in detail [10,11].

In this article, we attempt to understand the kinematics of geodesic flows in the presence of spacetime geometries representing black holes. Though, it is true that the Raychaudhuri equations have been around now for more than half a century, we are not aware of any attempt at a complete study of its solutions and the dependence of the ESR variables on the initial conditions imposed on them (however, see [12] for a recent work). A slight subtlety may be noted here. The Raychaudhuri equations are for the ESR variables, but they also involve the tangent vector field (denoted as u^i , later). Thus, unless one knows the solutions for the u^i (i.e., the first integrals of the geodesic equations) one cannot proceed towards solving for the ESR. Alternatively, one can try to find solutions for the full set of variables, i.e., u^i as well as the ESR, by imposing initial conditions on all of them and evolving the full system of equations along the flow. This approach enables us to obtain the tangent vector field as well as the ESR simultaneously. In our work, we adopt this method primarily for the four-dimensional cases where we are unable to solve for the geodesics or the u^i analytically.

As an aside, it may be noted, that the study of accretion of matter, or evolution of spacetime deformations near a black hole has been a fascinating topic of study in classical general relativity. Such processes can perhaps be investigated using the Raychaudhuri equations. The study of kinematics of non-spacelike congruences may further provide useful insights on the observable features in a given

*anir@mech.iitkgp.ernet.in

†hnandan@cts.iitkgp.ernet.in

‡sayan@cts.iitkgp.ernet.in

spacetime. We take this as a background motivation for our study.

The nontrivial geometry of different types of black holes is of crucial interest in general relativity and for our purpose, we will consider some typical two- and four-dimensional stringy black hole spacetimes. The two-dimensional black hole geometry we work with was first obtained in the context of string theory [13–16] in the nineties by Mandal *et al.* [17]. Exact solutions for geodesics and geodesic deviation in this two-dimensional stringy black hole background have already been studied earlier [18]. In four dimensions, the simplest eternal black hole geometry is, of course, the Schwarzschild. Rather than working with just the Schwarzschild alone, we consider the variations of the Schwarzschild which have arisen in the context of string theory [19–21]. All the four-dimensional geometries we choose to work with have a Schwarzschild limit (obtainable by setting a parameter in the line element to zero). Further, the validity of the various (weak, strong, null averaged) energy conditions for the matter that threads such stringy black hole spacetimes have also been investigated in detail in order to understand the nature of geodesic focusing [22].

Our article is organized as follows. We first review the background spacetimes (Sec. II) and then (Sec. III) derive the evolution (geodesic and Raychaudhuri) equations for the two-dimensional stringy black hole metric. In this 2D case, the Raychaudhuri equation is just the equation for the expansion scalar. We obtain analytical solutions for the expansion scalar, based on which the role of initial conditions on caustic formation and geodesic focusing/defocusing is investigated and analyzed. Subsequently (Sec. IV), we turn to actual four-dimensional solutions in dilaton-Maxwell gravity. We analyze the nature of deformations for the geodesic flows in the Garfinkle-Horowitz-Strominger (GHS) electric and magnetic (dual) solutions [19] and compare our results with those for Schwarzschild geometry (obtainable from the GHS metrics by setting a stringy parameter to zero). Here, the kinematics of deformations is studied on the two-dimensional equatorial plane. In the absence of analytical solutions, we solve the geodesic and Raychaudhuri equations numerically under differing initial conditions on the associated variables. The generic features of the evolution of deformations are brought out. The influence of the gravitational field on the evolution of the ESR is discussed and the effect of curvature is understood. Finally (Sec. V), we conclude our results and suggest some relevant future work.

II. THE STRINGY BLACK HOLE SPACETIMES

In this section, we quickly recall a well-known solution obtained in the context of two-dimensional low energy effective string theory [21]. The line element which we mention below solves the so-called β -function equations for the string σ model [21]. It is known that with appro-

priate methods of compactification one can obtain effective equations in two as well as other higher dimensions. These equations, in the simplest scenario, are for the metric field and the dilaton field. We quote below the line element in two dimensions [13,17],

$$ds^2 = -\left(1 - \frac{m}{r}\right)dt^2 + \frac{\kappa dr^2}{4r^2\left(1 - \frac{m}{r}\right)}; \quad (r \geq m), \quad (2.1)$$

where m and κ (with dimensions of length square) are the mass and central charge parameters, respectively, and are linked with the concepts in two-dimensional string theory [22] which we do not bother about here.

In $3 + 1$ dimensions, we also have asymptotically flat solutions representing black holes in dilaton-Maxwell gravity. Such solutions, due to Garfinkle, Horowitz, and Strominger [19], represent electric and dual magnetic black holes [20]. The spacetime geometry of these line elements are causally similar to Schwarzschild geometry. The metric for the black hole with electric charge is given as

$$ds^2 = -\frac{\left(1 - \frac{m}{r}\right)}{\left(1 + \frac{m \sinh^2 \alpha}{r}\right)^2} dt^2 + \frac{dr^2}{\left(1 - \frac{m}{r}\right)} + r^2 d\Omega_2^2, \quad (2.2)$$

where $d\Omega_2^2 = (d\psi^2 + \sin^2 \psi d\phi^2)$ is the metric on a two-dimensional unit sphere and α is a parameter related to the electric charge. Further, the dual (magnetic) metric of (2.2) is given as follows [20]:

$$ds^2 = -\frac{\left(1 - \frac{m}{r}\right)}{\left(1 - \frac{Q^2}{mr}\right)} dt^2 + \frac{dr^2}{\left(1 - \frac{m}{r}\right)\left(1 - \frac{Q^2}{mr}\right)} + r^2 d\Omega_2^2, \quad (2.3)$$

where Q is the magnetic charge of the black hole. In the respective limit of $\alpha = 0$ or $Q = 0$, we have Schwarzschild geometry in both the cases. We shall investigate the ESR variables for geodesic flows in each of the above two four-dimensional metrics and compare our results for the electric and magnetic solutions with those for the Schwarzschild.

For a general and compact representation of the above spacetimes, one can use a generic line element in $3 + 1$ dimensions as follows:

$$ds^2 = -X(r)dt^2 + Y(r)dr^2 + r^2 d\Omega_2^2, \quad (2.4)$$

for specific choices of $X(r)$ and $Y(r)$. The general structure of the geodesic equations for the line element (2.4) are given by

$$\ddot{i} + \frac{X'(r)}{X(r)} \dot{i} = 0, \quad (2.5)$$

$$\ddot{j} + \left(\frac{X'(r)\dot{i}^2 + Y'(r)\dot{r}^2 - 2r\dot{\psi}^2 - 2r\sin^2 \psi \dot{\phi}^2}{2Y(r)} \right) = 0, \quad (2.6)$$

$$\ddot{\psi} + \frac{2}{r} \dot{r} \dot{\psi} - \cos\psi \sin\psi \dot{\phi}^2 = 0, \quad (2.7)$$

$$\ddot{\phi} + \frac{2}{r} \dot{r} \dot{\phi} + 2 \cot\psi \dot{\psi} \dot{\phi} = 0, \quad (2.8)$$

where the prime denotes the differentiation with respect to r . Using the functional forms of $X(r)$ and $Y(r)$ [corresponding to the line elements (2.2) and (2.3)], in Eqs. (2.5) and (2.6), one can easily obtain the set of geodesic equations for the particular cases of the electric and magnetic stringy black holes. For the line element (2.1) in 1 + 1 dimensions, the term $r^2 d\Omega_2^2$ is absent in (2.4) and the geodesic equations are given by (2.5) and (2.6) (without the terms ψ and ϕ).

III. KINEMATICS OF DEFORMATIONS IN 1 + 1 DIMENSIONS

A. Kinematic variables

The evolution of spacelike deformations in a two-dimensional geodesic congruence is captured through the evolution of the geodesic deviation vector ξ^i (where $i = 1, 2$) on a spacelike hypersurface. These deformations can be described in terms of a second rank tensor $B_j^i = \nabla_j u^i$ [1,10], which governs the dynamics of the congruence. The second order derivative of the vector ξ^i with respect to an affine parameter is given as follows [10,11]:

$$\ddot{\xi}^i = (\dot{B}_j^i + B_k^i B_j^k) \xi^j. \quad (3.1)$$

The evolution tensor B_j^i in Eq. (3.1) is usually decomposed into irreducible parts signifying the expansion (scalar θ), shear (trace-free tensor σ_j^i), and rotation (antisymmetric tensor ω_j^i). Since $u_i \sigma_j^i = 0$ (spacelike deformations), and using the zero trace property, i.e., $\sigma_i^i = 0$, leads to $\sigma_0^0 = \sigma_1^1 = \sigma_2^2 = 0$. Similarly, the rotation tensor ω_j^i also satisfies $u_i \omega_j^i = 0$ which leads to $\omega_0^1 = \omega_1^0 = 0$. Therefore, the evolution tensor can be expressed only in terms of the expansion scalar, in the following form:

$$B_j^i = \theta h_j^i, \quad (3.2)$$

where the projection metric is defined as $h_j^i = \delta_j^i + u^i u_j$. Here, u_i is a timelike vector field.

B. The evolution equations

The evolution equations for a congruence of timelike geodesics for the present case consist of the Raychaudhuri equation for the expansion scalar and the geodesic equations derived for a particular metric. In order to derive the Raychaudhuri equation for the expansion scalar, we first write down the second derivative of the deformation vector in the following form:

$$\ddot{\xi}^i = -R^i_{lm} u^l u^m \xi^j. \quad (3.3)$$

1. Raychaudhuri equation for expansion scalar

Using the Eqs. (3.2) and (3.3) in the Eq. (3.1), one can now obtain the Raychaudhuri equation for the expansion scalar as given below:

$$\dot{\theta} + \theta^2 = -R^i_{lm} u^l u^m = -R_{lm} u^l u^m. \quad (3.4)$$

The general form of Eq. (3.4) for the metric (2.1) can also be written as follows:

$$\dot{\theta} + \theta^2 - \frac{R}{2} = 0, \quad (3.5)$$

where the Ricci scalar $R = 4m/\kappa r$. It may be noted that for $r \rightarrow \infty$, the Eq. (3.5) reduces to that in flat space without shear and vorticity. This evolution Eq. (3.5) along with the geodesic equations corresponding to the metric (2.1), form a complete set of equations required for studying the kinematics of deformations of geodesic congruences.

2. First integrals of geodesic equations

The first integrals of the geodesic equations in 1 + 1 dimensions can be obtained as

$$\dot{t} = \frac{E}{2(1 - \frac{m}{r})}, \quad (3.6)$$

$$\dot{r}^2 = \frac{1}{\kappa} [(E^2 - 4)r^2 + 4mr] = -V_2(r), \quad (3.7)$$

where $V_2(r)$ is an effective potential. It may be noted that the constraint $g_{\alpha\beta} u^\alpha u^\beta = -1$ (timelike geodesics) is used to obtain (3.7). The different choices for the constant of motion E result in the different behavior of the effective potential. One can have a harmonic, or an inverted harmonic oscillator corresponding to $E^2 < 4$, or $E^2 > 4$, respectively, while $E^2 = 4$ results in a linear potential with negative slope [18]. We will now solve the Raychaudhuri equation for the expansion scalar for all the choices of E mentioned above.

C. Exact solution for expansion scalar

The Eq. (3.5) can be solved for the above-mentioned three different cases by integrating Eq. (3.7) once (see [18]), and then using r in Eq. (3.5).

Case (A) $E^2 < 4$.

The Eq. (3.5) for the expansion scalar with $E^2 < 4$ reads

$$\ddot{\bar{\theta}}(\bar{\lambda}) + \bar{\theta}^2(\bar{\lambda}) - 2\sec^2 \bar{\lambda} = 0, \quad (3.8)$$

where we have used the scaling $\{\bar{\lambda}, \bar{\theta}\} = [(4 - E^2)/4\kappa]^{1/2} \{\lambda, \theta\}$. The solution of Eq. (3.8) is then given by

$$\bar{\theta}(\bar{\lambda}) = \frac{\tan \bar{\lambda} + (D_1 + \bar{\lambda}) \sec^2 \bar{\lambda}}{1 + (D_1 + \bar{\lambda}) \tan \bar{\lambda}}, \quad (3.9)$$

where D_1 is an integration constant which can be given in terms of the initial conditions as follows,

$$D_1 = \frac{(1 - \bar{\lambda}_0 \bar{\theta}_0) \tan \bar{\lambda}_0 + \bar{\lambda}_0 \sec^2 \bar{\lambda}_0 - \bar{\theta}_0}{\bar{\theta}_0 \tan \bar{\lambda}_0 - \sec^2 \bar{\lambda}_0}. \quad (3.10)$$

Case (B) $E^2 = 4$.

The equation for expansion scalar with $E^2 = 4$ reads

$$\dot{\theta}(\lambda) + \theta^2(\lambda) - \frac{2}{\lambda^2} = 0, \quad (3.11)$$

and the solution of Eq. (3.11) can be given as follows:

$$\theta(\lambda) = \frac{2D_2 \lambda^3 - 1}{\lambda(D_2 \lambda^3 + 1)}, \quad (3.12)$$

where the integration constant D_2 is given as

$$D_2 = -\frac{(1 + \lambda_0 \theta_0)}{\lambda_0^3 (\lambda_0 \theta_0 - 2)}. \quad (3.13)$$

Case (C) $E^2 > 4$.

The equation for the expansion scalar for this case reads

$$\ddot{\bar{\theta}}(\bar{\lambda}) + \bar{\theta}^2(\bar{\lambda}) - 2 \operatorname{cosech}^2 \bar{\lambda} = 0, \quad (3.14)$$

where $\{\bar{\lambda}, \bar{\theta}\} = [(E^2 - 4)/4\kappa]^{1/2} \{\lambda, \theta\}$. The solution of Eq. (3.14) is

$$\bar{\theta}(\bar{\lambda}) = \frac{\operatorname{coth} \bar{\lambda} - (D_3 + \bar{\lambda}) \operatorname{cosech}^2 \bar{\lambda}}{(D_3 + \bar{\lambda}) \operatorname{coth} \bar{\lambda} - 1}, \quad (3.15)$$

where the integration constant D_3 is given as

$$D_3 = \frac{(1 - \bar{\lambda}_0 \bar{\theta}_0) \operatorname{coth} \bar{\lambda}_0 - \bar{\lambda}_0 \operatorname{cosech}^2 \bar{\lambda}_0 + \bar{\theta}_0}{\bar{\theta}_0 \operatorname{coth} \bar{\lambda}_0 + \operatorname{cosech}^2 \bar{\lambda}_0}. \quad (3.16)$$

It is in order to mention here that, following an altogether different approach, one can calculate the expansion scalar θ as a function of r from the expressions of the first integrals $u^i = (\dot{t}, \dot{r})$ (the velocity field) given by (3.6) and (3.7) (i.e., without integrating the Raychaudhuri equation). Using $\theta = \nabla_i u^i$, we have

$$\theta = -\frac{2m}{\kappa \dot{r}} = \mp \frac{2m}{\sqrt{\kappa[(E^2 - 4)r^2 + 4mr]}}. \quad (3.17)$$

In view of the solutions of θ obtained earlier in this section by integrating the Raychaudhuri equation, the expression in (3.17) deserves attention. This expression for θ shows that a caustic forms at a turning point of the geodesic motion (i.e., where $\dot{r} = 0$). For $\dot{r} \rightarrow 0^+$ ($\dot{r} \rightarrow 0^-$), we have focusing (defocusing). In order to obtain the explicit λ dependence of θ , one has to substitute $r(\lambda)$ in (3.17) from the solution of the geodesic equation for r . It may be easily checked that the solutions thus obtained from (3.17) are special cases of the previous solutions. It is important to note that, unlike the solutions of θ obtained by integrating the Raychaudhuri equation, in the expression (3.17), there is no way of specifying any initial condition on θ . Thus, using (3.17), one cannot study the effect of initial conditions on the evolution of a geodesic congruence. This is a

subtle issue which will be discussed further in the following section.

D. Analysis of geodesic focusing

From the exact solutions of the expansion scalar obtained above by integrating the Raychaudhuri equations, one can determine the occurrence of finite time singularity (i.e., caustic formation). For Case (A), it may be deduced from (3.9) that the expansion scalar $\bar{\theta} \rightarrow \pm\infty$ as $\bar{\lambda} \rightarrow \pi/2$. Thus, we may have focusing or defocusing of geodesic congruences depending on the initial conditions. One may therefore calculate a critical initial value of the expansion scalar by exploiting the indefiniteness condition on θ which leads to $D_1 = -\pi/2$ (for $\bar{\lambda}_0 < \pi/2$). Now from (3.10), one can calculate the critical initial value of the expansion scalar as

$$\bar{\theta}_0^c = \frac{(\frac{\pi}{2} - \bar{\lambda}_0) \sec^2 \bar{\lambda}_0 - \tan \bar{\lambda}_0}{(\frac{\pi}{2} - \bar{\lambda}_0) \tan \bar{\lambda}_0 - 1}, \quad \left(\bar{\lambda}_0 < \frac{\pi}{2}\right). \quad (3.18)$$

From this analysis and using $\bar{\lambda}_0 = 1$, we have $\bar{\theta}_0^c \sim -1.95$. Thus, for $\bar{\theta}_0 < \bar{\theta}_0^c$, we have the congruence focusing, i.e., a finite time singularity occurs.

In Case (B), it may easily be concluded that caustic in the geodesic congruence forms for any initial condition $\theta_0 < -1/\lambda_0$. In this case, we have geodesic focusing whenever the initial condition satisfies this condition.

For Case (C), it may be observed from the solution (3.14) that defocusing is not possible. However, focusing can occur for an appropriate choice of initial conditions which can be obtained by choosing $\bar{\theta}_0 < \bar{\theta}_0^c$ where $\bar{\theta}_0^c = -2/\sinh 2\bar{\lambda}_0$ is the critical value of the initial expansion scalar. For $\bar{\theta}_0 > \bar{\theta}_0^c$, finite time singularity cannot occur.

It is well known from the work of Tipler [23] that if $R_{lm} u^l u^m \geq 0$ (timelike convergence condition) then focusing (and conjugate points) arise in the congruence within a finite value of the affine parameter. From our above analysis, it may thus seem counterintuitive that $R_{lm} u^l u^m = -R/2 \leq 0$ leads to focusing of timelike geodesic congruences in two-dimensional spacetimes. This, however, is not in conflict with the results of Tipler. In situations, such as those presented above, the timelike convergence condition is clearly violated. But, with appropriate initial conditions on the expansion (as shown above), one may still have a focusing of geodesic congruences. Therefore, we may say that initial conditions have a crucial role to play in focusing.

The Case (C) (i.e., with $E^2 > 4$) brings out a subtle and interesting difference between the solutions of θ in (3.14) and (3.17). As is clear from the expression of the effective potential in (3.7), all outward trajectories (outside the horizon) escape out to infinity without any turning point. Hence, one may conclude from (3.17) that there are no caustics in such a scenario. However, from the solution (3.14) discussed above, we do have focusing depending on the initial condition θ_0 . This difference can be reconciled

with if we realize that the expression (3.17) actually yields the expansion scalar field corresponding to the (static) velocity vector field $u^i = (t, \dot{r})$. On the other hand, the expression (3.14) tells us about the expansion history of a congruence, which may have been started with an arbitrary initial expansion, as observed in the local frame of a freely falling observer. This is also the approach adopted while proving the well-known focusing theorem [1–3].

IV. KINEMATICS OF DEFORMATIONS IN 3 + 1 DIMENSIONS

A. The evolution equations

In four dimensions, for a congruence of timelike geodesics, the transverse metric on a spacelike hypersurface can be expressed as

$$h_{\alpha\beta} = g_{\alpha\beta} + u_\alpha u_\beta, \quad (\alpha, \beta = 0, 1, 2, 3), \quad (4.1)$$

where u^α is the timelike vector field tangent to the geodesic at each point satisfying $u_\alpha u^\alpha = -1$, and the four-dimensional metric $g_{\alpha\beta}$ is defined through the line elements (2.2) and (2.3). The transverse metric satisfies $u^\alpha h_{\alpha\beta} = 0$, i.e., $h_{\alpha\beta}$ is orthogonal to u^α . This transverse spacelike hypersurface represents the local rest frame of a freely falling observer in the given spacetime. The point of interest in this investigation is to determine the deformations in this local rest frame as perceived by the observer. The evolution of spacelike deformations on this transverse hypersurface can be quantified using the tensor $B_{\alpha\beta}$, which can now be decomposed as follows:

$$B_{\alpha\beta} = \frac{1}{3}\theta h_{\alpha\beta} + \sigma_{\alpha\beta} + \omega_{\alpha\beta}, \quad (4.2)$$

where $\theta = B^\alpha_\alpha$ is the expansion scalar, while $\sigma_{\alpha\beta} = B_{(\alpha\beta)} - \theta h_{\alpha\beta}/3$ and $\omega_{\alpha\beta} = B_{[\alpha\beta]}$ are the shear and rotation tensors. The brackets $()$ and $[\]$ denote symmetrization and antisymmetrization, respectively. The shear and rotation tensors also satisfy $h^{\alpha\beta}\sigma_{\alpha\beta} = 0$ and $h^{\alpha\beta}\omega_{\alpha\beta} = 0$, as can be easily checked. The evolution equation for $B_{\alpha\beta}$ takes the form

$$\dot{B}_{\alpha\beta} + B_{\alpha\gamma}B^\gamma_\beta = -R_{\alpha\eta\beta\delta}u^\eta u^\delta. \quad (4.3)$$

Using this equation, one can now obtain the evolution equations for the ESR variables which are discussed below.

1. Raychaudhuri equations

Following well-known methods, the Raychaudhuri equations for the expansion scalar, and the shear and rotation tensors can be obtained as

$$\dot{\theta} + \frac{1}{3}\theta^2 + (\sigma^2 - \omega^2) + R_{\alpha\beta}u^\alpha u^\beta = 0, \quad (4.4)$$

$$\dot{\sigma}_{\alpha\beta} + \frac{2}{3}\theta\sigma_{\alpha\beta} + \sigma_{\alpha\gamma}\sigma^\gamma_\beta + \omega_{\alpha\gamma}\omega^\gamma_\beta - \frac{1}{3}(\sigma^2 - \omega^2)h_{\alpha\beta} + C_{\alpha\eta\beta\delta}u^\eta u^\delta - \frac{1}{2}\tilde{R}_{\alpha\beta} = 0, \quad (4.5)$$

$$\dot{\omega}_{\alpha\beta} + \frac{2}{3}\theta\omega_{\alpha\beta} + \sigma_\alpha^\gamma\omega_{\gamma\beta} + \omega_\alpha^\gamma\sigma_{\gamma\beta} = 0, \quad (4.6)$$

where $\sigma^2 = \sigma_{\alpha\beta}\sigma^{\alpha\beta}$, $\omega^2 = \omega_{\alpha\beta}\omega^{\alpha\beta}$, $\tilde{R}_{\alpha\beta} = h_{\alpha\gamma}h_{\beta\delta}R^{\gamma\delta} - h_{\alpha\beta}h_{\gamma\delta}R^{\gamma\delta}/3$, and $C_{\alpha\beta\eta\delta}$ is the Weyl tensor. These equations are first-order, coupled, nonlinear and inhomogeneous differential equations. The Eq. (4.4) for the expansion is the well-known Riccati equation, and, as mentioned before, is of prime importance in the context of the proof of the singularity theorems in general relativity [8,9] and in establishing the notion of geodesic focusing [6]. With the projection metric defined in (4.1), the Raychaudhuri equations essentially turn out to be structurally similar as in the case of three spatial dimensions. It may also be noted that there can be some congruences having a vanishing vorticity for which the velocity vector field is hypersurface orthogonal, and (4.6) becomes identically zero.

2. First integrals of geodesic equations on the equatorial section

One may note that the Eqs. (2.7) and (2.8) are independent of $X(r)$, $Y(r)$, and their derivatives. Without the loss of generality, one can choose $\psi = \pi/2$ which satisfies (2.7) identically. With this choice, we can capture the kinematics of deformations in the r - ϕ plane. One can now integrate (2.8) once to obtain $\dot{\phi} = C/r^2$, where C is a constant of motion. We will hereafter use these considerations. It is also noteworthy that with $\psi = \pi/2$, this four-dimensional description reduces to a three-dimensional one and the Raychaudhuri equations for the components of shear and rotation can be calculated in a way similar to our recent work (see Ref. [10]). In addition, we must keep in mind that the timelike vector field u^i satisfies the normalization condition $u^i u_i = -1$, which leads to

$$r^2[-X(r)\dot{t}^2 + Y(r)\dot{r}^2 + 1] + C^2 = 0. \quad (4.7)$$

The above constraint (4.7) also represents a first integral of the set of geodesic equations (2.5), (2.6), (2.7), and (2.8) for a specific choice of the constant of integration. We will now discuss the geodesic equations and effective potentials for the cases corresponding to the line elements (2.2) and (2.3), respectively.

Case I [corresponding to line element (2.2)]. The first integral of Eq. (2.5) for this case is calculated as follows:

$$\dot{t} = \frac{E(r + m\sinh^2\alpha)^2}{2r(r - m)}. \quad (4.8)$$

Now, using (4.8) in the constraint (4.7) leads to

$$i^2 = \frac{1}{4r^2} \left[E^2(r + m \sinh^2 \alpha)^2 + 4mr - 4r^2 + \frac{4C^2}{r}(m - r) \right] = -V_4^E(r), \quad (4.9)$$

where $V_4^E(r)$ is the effective potential for the case of an electric black hole. The effect of the parameter α on the radial motion for different values of E and C can be visualized directly from (4.9). The orbits (circular, scattering, and plunge) appear to be qualitatively similar to those in Schwarzschild geometry (see [24]).

Case II [corresponding to line element (2.3)]. The first integral of Eq. (2.5) for the magnetic case is as follows:

$$i = \frac{E(mr - Q^2)}{2m(r - m)}. \quad (4.10)$$

The constraint (4.7) along with Eq. (4.10) then leads to

$$i^2 = \frac{1}{4r^2} \left[E^2 r^2 + \frac{mr}{(mr - Q^2)} \times \left(4mr - 4r^2 + \frac{4C^2}{r}(m - r) \right) \right] = -V_4^M(r), \quad (4.11)$$

where $V_4^M(r)$ is the effective potential for the magnetic black hole. The structure of orbits are qualitatively same as in Case I.

The causal structure of the electric and magnetic stringy black hole spacetimes is similar to the Schwarzschild geometry [20]. This provides a motivation for comparing these three cases. The Schwarzschild metric can be constructed from (2.4) with $X(r) = (1 - m/r)$ and $Y(r) = (1 - m/r)^{-1}$, where usually $m = 2M$ with M as the mass of the Schwarzschild black hole. Later, we will consider $m = 1$ for numerical computations. The Raychaudhuri equations in the Schwarzschild case follow from (4.4), (4.5), and (4.6) with $R_{\alpha\beta}u^\alpha u^\beta = 0$ and $\tilde{R}_{\alpha\beta} = 0$. The geodesic equations are well known and the first integrals of the t and ϕ equations are same as those for the stringy black holes in 3 + 1 dimensions (see Sec. IVA 2) with $\psi = \pi/2$. The first integral of the r equation which satisfies the timelike constraint (4.7) on the velocity field leads to the following effective potential:

$$V_4^S(r) = -\frac{1}{4r^2} \left[(E^2 - 4)r^2 + 4mr + \frac{4C^2}{r}(m - r) \right]. \quad (4.12)$$

Since the Schwarzschild metric reduces to that of the flat spacetime for $r \rightarrow \infty$, the kinematics of deformations far from the singularity is same as for a static flat spacetime, a case which has already been well studied (see [11]). It may be noticed that the potential (4.9) [or (4.11)] reduces to (4.12) for $\alpha = 0$ (or $Q = 0$). The effective potentials are graphically presented in Fig. 1 (for $E = 1.95$) and in Fig. 2 (for $E = 2.01$).

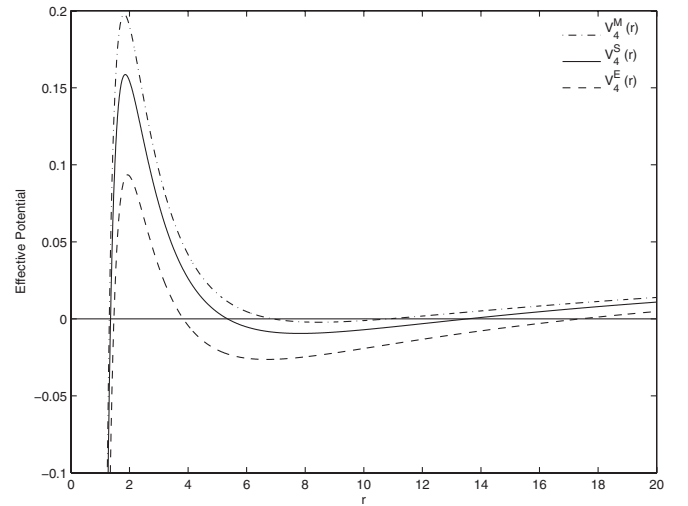


FIG. 1. Effective potentials for magnetic ($V_4^M(r)$, $Q = 0.25$), Schwarzschild ($V_4^S(r)$), and electric ($V_4^E(r)$, $\alpha = 0.25$) black holes with $E = 1.95$ and $C = 2.2$.

For the potential in Fig. 1, one can have bound or infalling trajectories (depending on the value of r_0), while the potential in Fig. 2 allows infalling and unbounded trajectories. Such trajectories are observationally important and therefore, in the following, we study the kinematics of deformations, numerically, in the above-mentioned backgrounds.

B. Analysis of deformations in the equatorial section

In this section, we study the kinematics of deformations restricted to the equatorial section of the black hole background. Consider the $\psi = \pi/2$ section of the spacetime which is a 2 + 1 dimensional slice with an induced metric, say, $\gamma_{\alpha\beta}$. The timelike geodesic motion is now confined to

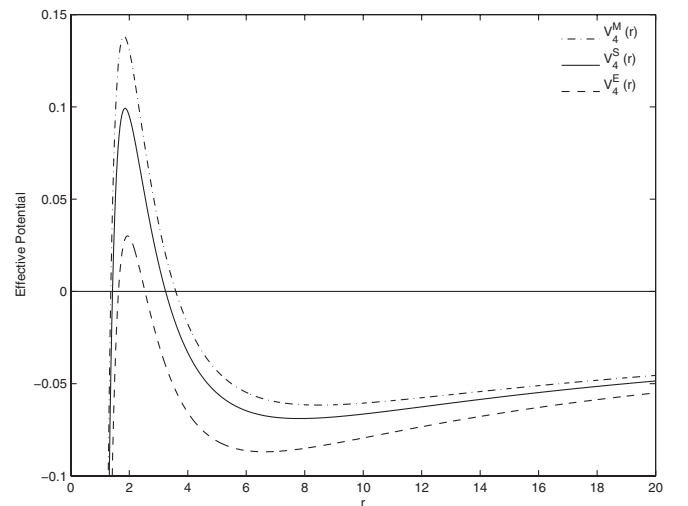


FIG. 2. Effective potentials for magnetic ($V_4^M(r)$, $Q = 0.25$), Schwarzschild ($V_4^S(r)$), and electric ($V_4^E(r)$, $\alpha = 0.25$) black holes with $E = 2.01$ and $C = 2.2$.

the $r - \phi$ plane. The geodesics of the induced metric are also geodesics of the full metric, and the effective potentials remain unaltered. We choose the deformations $\hat{\xi}^\alpha$ to be 2 + 1 dimensional and accordingly we define $\hat{B}_{\alpha\beta} = \hat{\nabla}_\beta \hat{u}_\alpha$, where $\hat{u}^\alpha \equiv (i, \dot{r}, \dot{\phi})$. One can now define the projection tensor $\hat{h}_{\alpha\beta} = \gamma_{\alpha\beta} + \hat{u}_\alpha \hat{u}_\beta$.

We then consider a freely falling (Fermi) normal frame E_μ^α (with $E_r^\alpha = \hat{u}^\alpha$) which is parallelly transported according to $\hat{u}^\alpha \hat{\nabla}_\alpha E_\mu^\beta = 0$. The kinematics of deformations, restricted to the two-dimensional spacelike hypersurface (the local frame of a freely falling observer) in this basis, can now be represented by four kinematical quantities, namely, θ , σ_+ , σ_\times , and ω . The tensor $\hat{B}_{\alpha\beta}$ in this basis, can be constructed as

$$\hat{B}_{\alpha\beta} = \left(\frac{1}{2}\theta + \sigma_+\right)e_\alpha^r e_\beta^r + \left(\frac{1}{2}\theta - \sigma_+\right)e_\alpha^\phi e_\beta^\phi + (\sigma_\times + \omega)e_\alpha^r e_\beta^\phi + (\sigma_\times - \omega)e_\alpha^\phi e_\beta^r, \quad (4.13)$$

where e_α^μ are coframe basis satisfying $e_\alpha^\mu E_\nu^\alpha = \delta_\nu^\mu$. The ESR can be extracted from the evolution tensor (4.13) using the basis vectors as follows:

$$\theta = \hat{B}_{\alpha\beta} \hat{h}^{\alpha\beta} \equiv \hat{B}_{\alpha\beta} \gamma^{\alpha\beta}, \quad (4.14)$$

$$\sigma_+ = \frac{1}{2}(\hat{B}_{\alpha\beta} E_r^\alpha E_r^\beta - \hat{B}_{\alpha\beta} E_\phi^\alpha E_\phi^\beta), \quad (4.15)$$

$$\sigma_\times = \frac{1}{2}(\hat{B}_{\alpha\beta} E_r^\alpha E_\phi^\beta + \hat{B}_{\alpha\beta} E_\phi^\alpha E_r^\beta), \quad (4.16)$$

$$\omega = \frac{1}{2}(\hat{B}_{\alpha\beta} E_r^\alpha E_\phi^\beta - \hat{B}_{\alpha\beta} E_\phi^\alpha E_r^\beta). \quad (4.17)$$

As in the 1 + 1 dimensional example discussed earlier, the first integrals of the geodesic equations of the 2 + 1 dimensional line element enable us to find the expansion, shear, and rotation for a geodesic congruence. Making use of the vector field \hat{u}^α and the definition of $\hat{B}_{\alpha\beta}$, we can obtain θ , for example, as follows:

$$\begin{aligned} \theta &= \pm \frac{1}{\dot{r}XY} \left[\frac{E^2}{4r} - \frac{X}{r} - (r^2 + C^2) \frac{X'}{2r^2} \right] \\ &= \pm \frac{1}{XY} \frac{\frac{E^2}{4r} - \frac{X}{r} - (r^2 + C^2) \frac{X'}{2r^2}}{\sqrt{\frac{E^2}{4XY} - (r^2 + C^2) \frac{1}{r^2 Y}}}, \end{aligned} \quad (4.18)$$

where $X(r)$ and $Y(r)$ are the metric functions defined earlier. Similar general expressions for σ_+ , σ_\times , and ω can also be obtained. It may be noted that the expressions thus obtained are all functions of r . Obtaining $r(\lambda)$ by solving the geodesic equations, one can then find $\theta(\lambda)$, $\sigma_{ij}(\lambda)$, and $\omega_{ij}(\lambda)$. From all these expressions, it is easy to state that

divergences in the ESR appear at the turning points (i.e., where $\dot{r} = 0$). Similarly as in 1 + 1 dimensions, these solutions represent only special solutions with special initial conditions. They do not reveal the effect of initial conditions on the evolution of the ESR variables. A more general class of solutions corresponding to arbitrary initial conditions on the ESR variables are obtained by integrating the full set of Raychaudhuri equations together with the geodesic equations.

In order to understand the caustic formation/focusing behavior in more detail, let us redefine the expansion scalar as $\theta = 2\dot{F}/F$, where the dot indicates the derivative with respect to λ . One may then use the Fermi normal basis to rewrite (4.4) as the following Hill-type equation:

$$\ddot{F} + HF = 0, \quad (4.19)$$

where $H = \sigma_+^2 + \sigma_\times^2 - \omega^2 + G$ and $G = R_{\alpha\beta} u^\alpha u^\beta / 2$. The notion of caustic formation due to focusing is related to $F = 0$, $\dot{F} < 0$ at a finite λ . This can be achieved under specific conditions on (a) the sign of H , and (b) the initial values of the ESR. For a complete analysis, we would be required to consider all possible initial values (positive, negative, or zero) for the ESR and H . Here, we restrict ourselves to some special cases and briefly comment on the rest.

- (A) If $H > 0$ for all λ , then conjugate points exist and focusing takes place, as is well known.
- (B) When $H < 0$ for all λ , we have focusing only when $\theta_0 < \theta_0^c < 0$. When $\theta_0 > \theta_0^c$, there is defocusing.
- (C) If H is sign indefinite over the range of λ , then there may be various possibilities depending on the initial conditions of the ESR.

The conclusion (B) has already been illustrated above for the 1 + 1 dimensional case in Sec. III.

We now illustrate the above conclusions with our numerical evaluations and corresponding plots for the ESR variables. In what follows, we analyze and compare the kinematics of deformations in the charged (electric and magnetic) stringy black hole with the Schwarzschild black hole. For this, we consider the two potentials shown in Figs. 1 and 2 for the bound and escaping trajectories for the reason mentioned before. Corresponding to these two potentials, the ESR variables for the two black holes are compared below. In both the cases, the initial radius is taken as $r_0 = 8$. The initial \dot{r} is considered as positive for the evaluations for Fig. 3, while \dot{r} is taken as negative for the evaluations depicted in Fig. 6. In these figures, the variation of the invariants θ , $\sigma^2 = \sigma_+^2 + \sigma_\times^2$, and ω are presented and compared for the corresponding black hole backgrounds.

In Fig. 3 (corresponding to the potential shown in Fig. 1), we observe geodesic focusing in all the three backgrounds. In order to understand this behavior in light of the general conclusions mentioned earlier, we have plotted H and G in Fig. 4, for geodesic congruences in

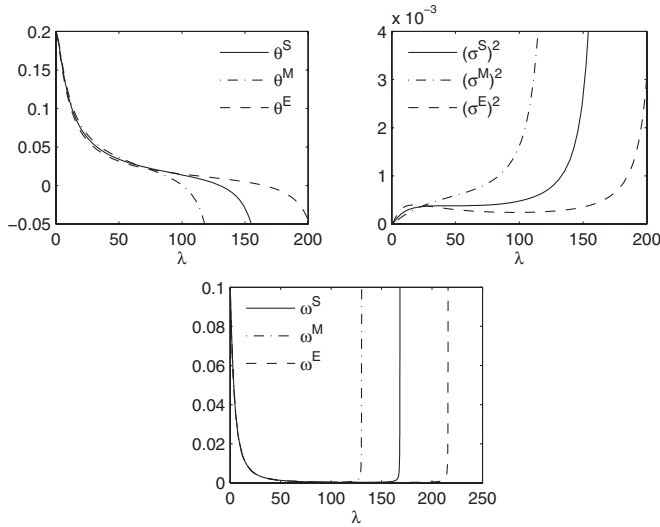


FIG. 3. Comparison of ESR variables in electric ($\alpha = 0.25$), magnetic ($Q = 0.25$), and Schwarzschild black holes with $E = 1.95$, $C = 2.2$, $\theta_0 = 0.2$, $\sigma_{+0} = 0$, $\sigma_{\times 0} = 0$, $\omega_0 = 0.1$, and $r_0 = 8$.

the electric and magnetic stringy black holes. It is evident that G is negative definite along the geodesic flow. However, H is initially negative over a certain range of λ but soon turns positive and increases monotonically due to dominating contributions from the shear components. Thus, one may say that the focusing effect seen here is largely shear induced. Even though the rotation term appears with an opposite sign in $H(\lambda)$, its net value beyond a certain λ becomes positive and may be responsible for the focusing effect. We may note, in passing, that the focusing effect in Schwarzschild spacetime is entirely due the eventual dominance of shear over rotation.

The time of approach to a singularity in the congruence, which we denote by λ_s , can also be an interesting quantifier which we can use to characterize geodesic flows in the three backgrounds. We have numerically studied the effect of the initial expansion θ_0 on λ_s for the different black hole

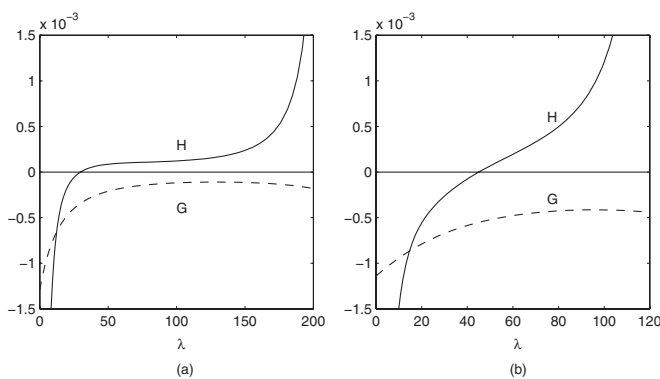


FIG. 4. Variation of G and H for (a) electric and (b) magnetic black holes with the initial conditions as for Fig. 3.

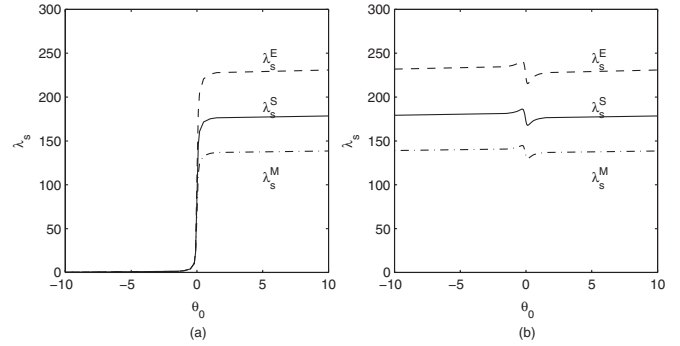


FIG. 5. Variation of time to singularity (λ_s) versus initial expansion (θ_0) for different black hole metrics (a) without initial rotation of the congruence, and (b) with initial rotation of the congruence ($\omega_0 = 0.1$). Here, we have considered $\sigma_{+0} = 0$ and $\sigma_{\times 0} = 0$.

metrics without and with initial rotation ω_0 of the congruence. The results of this study are shown in Fig. 5. It is interesting to note that for an initially contracting congruence the singularity occurs more rapidly as compared to an initially expanding congruence. Furthermore, the time to singularity does not change appreciably for large values of initial expansion/contraction. On the other hand, even with a small initial rotation ($\omega_0 = 0.1$), λ_s remains almost unchanged over the whole range of variation of the θ_0 considered. It was also found (though the results are not presented) that, with initial shear, λ_s reduces drastically over the complete range of θ_0 which is also expected qualitatively (see [6]). One difference that emerges from this study on the three black hole metrics considered is that $\lambda_s^E > \lambda_s^S > \lambda_s^M$ as observed in Fig. 5.

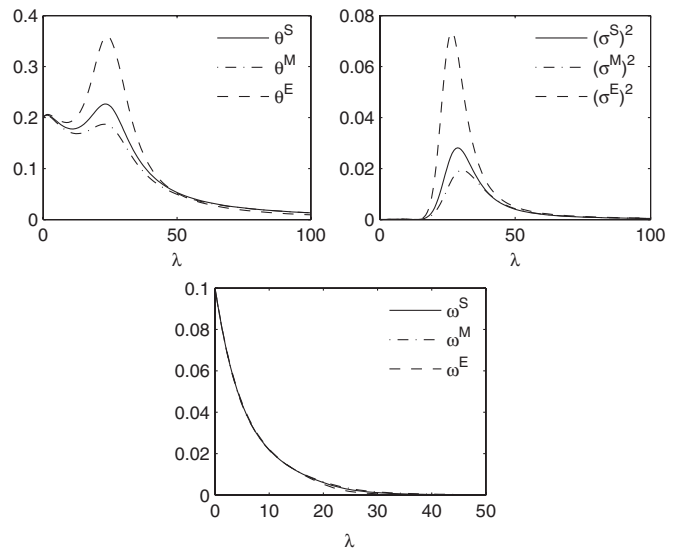


FIG. 6. Comparison of ESR variables in electric ($\alpha = 0.25$), magnetic ($Q = 0.25$), and Schwarzschild black holes with $E = 2.01$, $C = 2.2$, $\theta_0 = 0.2$, $\sigma_{+0} = 0$, $\sigma_{\times 0} = 0$, $\omega_0 = 0.1$, and $r_0 = 8$.

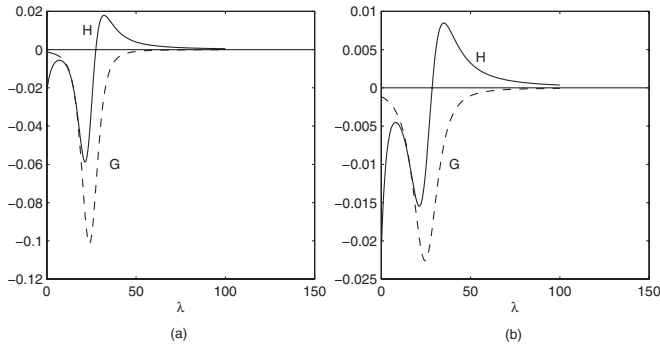


FIG. 7. Variation of G and H for (a) electric and (b) magnetic black holes with the initial conditions as for Fig. 6.

In Fig. 6 (corresponding to the potential shown in Fig. 2), there is no focusing. We observe from Fig. 7 that H is sign indefinite and bounded over the range of λ . As mentioned in (C) above, in such situations, definite conclusions are difficult to arrive at because of the sensitive dependence of the results on the initial values of the ESR. The following curious features may be associated with the no-focusing behavior observed above. First, it is easy to note from the Fig. 7 that $\int H d\lambda$ has a negative value, unlike that observed in Fig. 4. Further, the nature of H (and \dot{H}) in Figs. 4 and 7, for large λ , are distinctly different and may also be a cause of the no-focusing effect.

Additionally, the location (in λ) of the extrema (maxima/minima) in the ESR shifts to larger λ as we move from the electric to Schwarzschild to the magnetic solutions. This is evident in Fig. 6. If λ_e^E denotes the location of an extremum, from the figure, we can easily say that $\lambda_e^S > \lambda_e^M$.

Finally, it may be noted from the plots in Fig. 6 corresponding to ω that the rotation of the congruence is largely similar irrespective of the metric. This is expected since $\omega = \omega_0 \exp(-\int \theta dt)$, and the variation of θ is almost similar in the three backgrounds. In contrast, from this expression of ω , we note that the divergence (to $-\infty$) of θ is reflected in the divergence (to $+\infty$) of ω , as shown in Fig. 3.

V. SUMMARY AND CONCLUSIONS

In this article, we have investigated the kinematics of timelike geodesic flows in two- and four-dimensional spacetimes representing stringy black holes. We now briefly summarize the work done, the conclusions drawn from it, and also mention possibilities on future work.

- (i) The exact solutions of the expansion scalar for the different cases in 2D have been calculated by solving the corresponding Raychaudhuri equation for the expansion. The occurrence of a finite time singularity (i.e., caustic formation/geodesic focusing) in each case is then discussed with particular reference to the relation between initial conditions and the behavior of the expansion.

- (ii) The geodesic equations and the Raychaudhuri equations for the ESR are written out and solved numerically for timelike geodesic congruences in two different stringy black hole spacetimes in four dimensions.
- (iii) We have drawn some general conclusions and made some observations on geodesic focusing which we believe are new. In particular, we have demonstrated how different initial conditions on the ESR can affect the occurrence of geodesic focusing. We also show how focusing can be affected by the variation of $H(\lambda)$. Even in situations where the timelike convergence condition is violated, domination of shear can still lead to focusing. Further, we have introduced a new quantity—the time of approach to singularity, which may be used to distinguish between geodesic flows in different backgrounds. Though not presented in this article, we have observed that, in the presence of initial shear (i.e., $\sigma_{+0} \neq 0$ and/or $\sigma_{\times 0} \neq 0$), the time of approach to singularity (λ_s) is significantly reduced.
- (iv) In the scenario depicted in Fig. 6, where there is no focusing, we make an attempt towards understanding why this happens by analyzing the behavior. We observe here that the locations of the extrema show a systematic shift as we move from geodesic flows in the electric to the Schwarzschild and then to the magnetic black holes.
- (v) On the whole, in some sense, the stringy nature of the black hole geometry does seem to manifest itself in the nature of evolution of the ESR.

An interesting issue that is still left unanswered in this work is the role of duality of the electric and magnetic black hole metrics on the kinematics. The question that might be asked is whether the kinematics in these two spacetimes are also dual of one another in some sense. It may be tempting to approach this issue by searching relations between the parameters α , Q , m , E , and C which leaves the kinematics invariant.

The metrics of the stringy black holes have coordinate singularities at specific values of r and hence cannot be extended beyond. Thus, for a more complete description of the kinematics of flows, it will be interesting to study geodesic flows using a different, extendable coordinate system (viz. the maximally extended Kruskal coordinate system). Besides this, our work has so far focused entirely on timelike geodesics in static spacetimes. It would be worth studying the nature of null congruences in a similar fashion. A logical next step would be to consider geodesic flows in stationary metrics (such as the Kerr black hole and its generalizations).

Finally, the essential goal behind this work has been to demonstrate that the Raychaudhuri equations and the geodesic equations can be solved simultaneously to give us a complete picture of geodesics and geodesic flows in any

given spacetime. Thus, we have a viable approach for studying the kinematics of geodesic congruences for any given metric which can help us distinguish between spacetimes through the behavior of trajectories and families of trajectories. In the long run, it may be possible to make use of these results in arriving at distinct observable effects in specific gravitational fields.

ACKNOWLEDGMENTS

The authors thank the Department of Science and Technology (DST), Government of India for financial support through a sponsored project (Grant No. SR/S2/HEP-10/2005). The authors also thank the anonymous referee for his constructive comments which helped in improving the presentation of the paper.

-
- [1] E. Poisson, *A Relativists' Toolkit: The Mathematics of Black Hole Mechanics* (Cambridge University Press, Cambridge, UK, 2004).
 - [2] R.M. Wald, *General Relativity* (University of Chicago Press, Chicago, USA, 1984).
 - [3] P.S. Joshi, *Global Aspects in Gravitation and Cosmology* (Oxford University Press, Oxford, UK, 1997).
 - [4] G.F.R. Ellis, *General Relativity and Cosmology, International School of Physics, Enrico Fermi-Course XLVII* (Academic Press, New York, 1971).
 - [5] I. Ciufolini and J.A. Wheeler, *Gravitation and Inertia* (Princeton University Press, Princeton, USA, 1995).
 - [6] S. Kar and S. SenGupta, *Pramana* **69**, 49 (2007); arXiv:gr-qc/0611123 and references therein; S. Kar, *Resonance, Journal of Science Education* **13**, 319 (2008).
 - [7] S.W. Hawking and G.F.R. Ellis, *The Large Scale Structure of Spacetime* (Cambridge University Press, Cambridge, UK, 1973).
 - [8] R. Penrose, *Phys. Rev. Lett.* **14**, 57 (1965).
 - [9] S.W. Hawking, *Phys. Rev. Lett.* **15**, 689 (1965); **17**, 444 (1966).
 - [10] A. Dasgupta, H. Nandan, and S. Kar, *Ann. Phys. (N.Y.)* **323**, 1621 (2008); arXiv:0709.0582.
 - [11] A. Dasgupta, H. Nandan, and S. Kar, arXiv:0804.4089 [Int. J. of Geom. Meth. Mod. Phys. (to be published)].
 - [12] F. Shojai and A. Shojai, *Phys. Rev. D* **78**, 104011 (2008).
 - [13] E. Witten, *Phys. Rev. D* **44**, 314 (1991).
 - [14] A. Sen, *Phys. Rev. Lett.* **69**, 1006 (1992).
 - [15] D. Grumiller, W. Kummer, and D. V. Vassilevich, *Phys. Rep.* **369**, 327 (2002).
 - [16] J. Harvey and A. Strominger, in *String Theory and Quantum Gravity 92*, edited by J. Harvey *et al.* (World Scientific, Singapore, 1993).
 - [17] G. Mandal, A.M. Sengupta, and S.R. Wadia, *Mod. Phys. Lett. A* **6**, 1685 (1991).
 - [18] R. Koley, S. Pal, and S. Kar, *Am. J. Phys.* **71**, 1037 (2003).
 - [19] D. Garfinkle, G.T. Horowitz, and A. Strominger, *Phys. Rev. D* **43**, 3140 (1991); *Phys. Rev. D* **45**, 3888(E) (1992).
 - [20] G.T. Horowitz, arXiv:hep-th/9210119.
 - [21] M.S. Green, J.H. Schwarz, and E. Witten, *Superstring Theory* (Cambridge University Press, Cambridge, UK, 1987); J. Polchinski, *String Theory* (Cambridge University Press, Cambridge, UK, 1997).
 - [22] S. Kar, *Phys. Rev. D* **55**, 4872 (1997) and references therein.
 - [23] F.J. Tipler, *Phys. Rev. D* **17**, 2521 (1978); *Ann. Phys. (N.Y.)* **108**, 1 (1977).
 - [24] J.M. Hartle, *Gravity An Introduction to Einstein's General Relativity* (Pearson Education Inc., Singapore 2003).